Cellular solidification as a bifurcation problem

Peter Haug
Institute for Information Sciences, University of Tübingen, D-7400 Tübingen, Federal Republic of Germany
(Received 6 October 1986)

The spontaneous formation and evolution of stationary cellular interfaces arising in directional solidification of a binary alloy are discussed in terms of bifurcation theory. Algebraic bifurcation equations for the amplitudes of the cells are derived from the nonlinear equations of motion with the interface velocity as a control parameter. It is shown that the form of these bifurcation equations is determined by the system's symmetry and by nonflux boundary conditions imposed at the sidewalls. The generic transitions from planar to cellular interfaces and between cellular interfaces of different wavelengths are determined and the effects of variations of system parameters on the bifurcation diagrams are analyzed. A variety of new phenomena, such as various types of hysteresis and cellular island formation, secondary bifurcations describing beats and mode jumping among interfacial cells, and tertiary Hopf bifurcations to standing waves, is discovered, which one can expect to find in solidification experiments on purely topological grounds.

I. INTRODUCTION

The formation and evolution of spatio-temporal structures is the result of sudden qualitative changes, known as bifurcations. These occur in a nonlinear system if an externally controllable parameter passes through critical values so that a balance existing between competing system-immanent effects breaks down. As a consequence, an initially quiescent system becomes unstable and, in a sequence of bifurcations, restabilizes successively in ever more complex space- and time-dependent configurations. Thereby, an important role is played by geometrical constraints, for example, the dimension and shape of the underlying system, inherent symmetries and boundary conditions, which restrict the kinds of possible bifurcations. Within a particular symmetry constraint, the bifurcations occur in certain definite and classifiable ways. However, the behavior of a particular system is eventually determined by the underlying physics. The classifiability is a consequence of the fact that physical systems which allow reproducible experiments are structurally stable, i.e., that they are insensitive to small perturbations. In such systems an unstable event, i.e., a bifurcation, appears as a singular element within a stable process. This fact explains the qualitative similarity among the instabilities that lead to convective patterns in fluids,[1] cellular flame fronts,[2] and crystal growth,[3] chemical patterns,[4] and so forth.[5]

This paper deals with the problem of stationary cellular patterns formed by the interface between the solid and the liquid phase of a binary alloy in directional solidification.[6,3] The objective is to carry out a fully nonlinear analysis of the problem by determining the generic transitions from flat to cellular interfaces and between cellular interfaces of different wavelengths. The one-sided solidification model[6,3] is used as a paradigm. The main principle is to deal with the solutions of algebraic bifurcation equations for the amplitudes of bifurcating modes rather than with the equations of motion themselves. The latter have been studied by Mullins and Sekerka,[7] Wollkind and Segel,[6] Langer and Turski,[8] Langer,[9] and others,[10,11] while numerical simulations of interface profiles have been performed by Kerszberg,[12] McFadden and Coriell,[13] and by Ungar and Brown.[14] Introductions to both the experimental and theoretical sides of the subject and further references can be found in articles by Langer,[3] Trivedi and Somboonsuk,[15] Glicksman,[16] and Heslot and Libchaber.[17] What is needed at this point is an analytical and largely model-independent approach to the problem of cellular interface formation which starts from first principles and reveals the basic phenomena which one can expect to find in solidification experiments. An appropriate framework for this is provided by the theory of imperfect bifurcations.[18,19] This theory allows us to determine and to categorize all possible instabilities and bifurcations to stable stationary patterns that can occur in solidifying systems when a distinguished external control parameter varies. The formalism developed below accounts also for symmetry constraints and material parameter variations.

We begin, in Sec. II, by summarizing the basic equations which describe the one-sided, nonlinear model of directional solidification with the interface velocity considered as the externally controllable parameter. These equations are supplemented by nonflux (Neumann) boundary conditions at the sidewalls of the solidifying material. Using a general multimode approach, we derive bifurcation equations for cellular interfaces for the case in which one or two modes become unstable at critical values of the interface velocity. The form of these equations is essentially determined by the reflection symmetry of the equations of motion and by the boundary conditions. After a discussion of the associated linearized system we describe, in Sec. III A, the basic concepts and results of imperfect bifurcation theory and outline the geometrical reasoning that leads to a description of interface transitions in terms of bifurcation diagrams. The principal contents of our results are contained in Secs. III B and III C and are expressed by a set of perturbed bifurcation dia-

grams for the amplitudes of bifurcating cellular interfaces as functions of the interface velocity and of system parameters. Among the interesting phenomena we find primary bifurcations of a single mode exhibiting bistable and mushroom hysteresis and the appearance of islands not connected with the stationary state. This means that for certain parameter values there exist stable cellular interfaces without any instability of the plane interface being present. The simultaneous instability of two different modes leads to primary bifurcations representing single-mode solutions and to secondary bifurcations describing mixed-mode solutions which connect the single-mode branches. The mixed-mode solutions correspond to interfaces representing spatial beats of, and mode jumping between, two different wavelengths. In addition, tertiary bifurcations on the mixed-mode branches are found, i.e., Hopf-bifurcations to standing waves. In Sec. IV, we summarize our results and discuss some implications for further research.

II. DIRECTIONAL SOLIDIFICATION WITH NONFLUX BOUNDARY CONDITIONS

In this section we summarize the basic equations describing the one-sided model of directional soldification[3,6] subjected to nonflux boundary conditions. Then, using a general multimode approach, a reduction to amplitude equations for stationary cellular interfaces is carried out[12] and a linear stability analysis is performed.

A. The solidification model

Consider a long, thin sample of a dilute binary alloy of width L lying in the (ξ,η) plane which is drawn, at constant velocity V, through a fixed temperature gradient G established by stationary hot and cold contacts at A and B (Fig. 1). The temperatures are chosen so that the sample is molten at A and solid at B with the solid-liquid interface visible in between. We assume that diffusion of the solute on the solid side of the interface is negligible (one-sided model), that the latent heat, which is released at the interface, is small, and that convection in the liquid can be neglected.[3,7] This implies that the solidification process is primarily governed by the solute transport in the liquid towards or away from the interface whose position is at $\eta=s(\xi,t)$. At low interface velocity V, the external thermal conditions impose a planar solidification front $s=0$. With increasing V, solute diffusion tends to destabilize the planar front: If the solid bulges, the concentration gradient is increased in front of the bulge and the solute current is enhanced so that the growth of the bulge is favored and the interface becomes unstable. This destabilizing effect of the concentration gradient is counterbalanced by the stabilizing effects of the surface tension and the temperature gradient. The resulting interplay between kinetic and capillary effects produces the complex patterns that we see in the advancing front as V increases, viz., planar interface, spatially periodic cellular states, and, finally, dendrites.

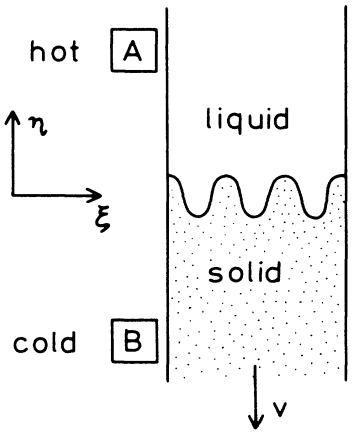

FIG. 1. Schematic representation of the directional solidification system.

In the frame of reference moving in the η direction at the interface velocity, the diffusion of the suitably normalized solute concentration $w(\xi,\eta,t)$ is determined by the equation[20]

$$w_{\xi\xi}+w_{\eta\eta}+vw_{\eta}-w_t=0 \tag{2.1}$$

for $0\leqq\xi\leqq b$, $\eta\geqq s(\xi,t)$. Here the subscripts indicate partial differentiation and v is the dimensionless interface velocity. Equation (2.1) is to be solved inside the liquid with the Gibbs-Thomson boundary condition on the interface $\eta=s(\xi,t)$

$$w=-s-\frac{1}{u}\mathscr{K}(s)\ , \tag{2.2}$$

and the Rankine-Hugoniot condition which relates the speed of diffusion to that of the interface, viz.,

$$s_t+v+w_{\eta}-s_{\xi}w_{\xi}=0,\quad \eta=s(\xi,t)\ . \tag{2.3}$$

In Eq. (2.2),

$$\mathscr{K}(s)=-s_{\xi\xi}/(1+s_{\xi}^2)^{3/2}$$

is the curvature of the interface at $\eta=s(\xi,t)$, and $u>0$ is a variable depending on the various physical parameters involved,

$$u=\tilde{m}^2c_{\infty}^2(1-\kappa_{\infty})^2/(T_0\tilde{\Gamma}G\kappa_{\infty}^2)\ ,$$

where c_{∞} is the solute concentration at infinity, T_0 the melting temperature of the planar interface, $\tilde{\Gamma}$ the capillary length, $\tilde{m}$ the slope of the liquidus line, and κ_{∞} is the segregation coefficient. In deriving (2.2) and (2.3) we have assumed that the concentration jump at the interface is constant and that the liquidus line in the phase diagram is linear.[3]

At the sidewalls of the sample we impose the boundary conditions for the concentration field

$$w_{\xi}=0\ \text{ for } \xi=0,\ \xi=b \tag{2.4}$$

and for $\eta\to\infty$ we have

$$w(\xi,+\infty,t)=-1\ . \tag{2.5}$$

The physically necessary nonflux (Neumann) boundary conditions (2.4) are often disregarded in solidification

models,[3,10] although, as we shall see, they are of considerable importance for the cellular bifurcation problem. Furthermore, we assume that the interface moves slowly in comparison to the speed of solute diffusion. This corresponds to a "quasistationary approximation,"[3] in which (2.1) is replaced by

$$w_{\xi\xi}+w_{\eta\eta}+vw_{\eta}=0 \ . \tag{2.6}$$

In virtue of (2.2), the system to be solved is highly nonlinear. The planar interface solution of (2.2)–(2.6) is given by

$$w_0(\xi,\eta,t)=\exp(-v\eta)-1, \quad s(\xi,t)=0 \ .$$

B. Bifurcation equations

In this section we derive equations of motion for the interfacial displacement $s(\xi,t)$ and by using the Lyapunov-Schmidt method which consists here simply of an application of the implicit function theorem, the infinite-dimensional problem of steady-state cellular bifurcation is reduced to a small number of algebraic equations. These contain all the information about the bifurcation behavior near the onset of instability. Differentiating (2.3) with respect to ξ yields, together with (2.4), at $\eta=s(\xi,t)$, $\xi=0,b$, the equation

$$s_{\xi}(w_{\eta\eta}-w_{\xi\xi})=0 \ . \tag{2.7}$$

Since $w_{\eta\eta}-w_{\xi\xi}=v^2\neq 0$ for the planar interface solution w_0, we obtain near the onset of instability

$$s_{\xi}=0 \tag{2.8}$$

at the sidewalls $\xi=0,b$. In virtue of (2.8), s can be represented by a cosine series

$$s(\xi,t)=\sum_{m=0}^{+\infty}\varepsilon_m(t)\cos(m\sqrt{u}\,k_0\xi) \ , \tag{2.9}$$

where $\varepsilon_m\in\mathbb{R}$ and

$$k_0=\pi/(b\sqrt{u}\,)=(\pi/L)(T_0\tilde{\Gamma}/G)^{1/2}>0$$

is the fundamental wave number, depending on the width L of the sample [the factor $\sqrt{u}$ in (2.9) has been introduced to simplify the analysis]. Since the ε_m vary with time, so do s and w. Hence w is a functional of the amplitudes ε_m, $w=w(\xi,\eta,t,\varepsilon)$ with $\varepsilon=(\varepsilon_0,\varepsilon_1,\varepsilon_2,\dots)$, which can be expanded into a formal Taylor series around the planar interface $\varepsilon=0$,[12,20]

$$w=\sum_{n=0}^{\infty}\sum_{|\mu|=n}D^{\mu}w\,|_{\varepsilon=0}\,\varepsilon^{\mu}/\mu! \tag{2.10}$$

with multi-indices μ. By determining the Taylor coefficients of (2.10) with (2.6), (2.2), and (2.5), and substituting the resulting formal Taylor series (2.10) into equation (2.3), we obtain an equation of motion for the interface s in the form of an infinite system of first-order evolution equations for the $\varepsilon_i(t)$[12]

$$\dot{\varepsilon}_i=\sum_{j=1}^{\infty}\sum_{\substack{i_1,i_2,\dots,i_j\in Z\\ i_1\leq i_2\leq\cdots\leq i_j\\ \sum_k i_k=i}}a^{(i)}_{i_1,i_2,\dots,i_j}\varepsilon_{|i_1|}\varepsilon_{|i_2|}\cdots\varepsilon_{|i_j|} \ , \tag{2.11a}$$

i.e.,

$$\dot{\varepsilon}_i=a_i\varepsilon_i+M_i(\varepsilon), \quad i=0,1,2,\dots \tag{2.11b}$$

where $a_i\equiv a_i^{(i)}$ and M_i describe the nonlinear effects and the $a_i^{(i)}$ (Sec. II C) are real.

The coefficients $a^{(n)}_{n_1,n_2,\dots,n_m}$ (cf. the Appendix), which depend on v and on the system parameters u and k_0, can be calculated to any desired order using computer algebraic symbolic manipulation systems.[20] The trivial solution $\varepsilon=0$ of (2.11) describes the planar interface. It is stable if $a_i<0$ for all i which is the case for sufficiently small v (Sec. III C). As v increases and passes through a critical value v_c, some of the eigenvalues a_i of the linearized system (2.11) go through zero from negative values. Then the planar interface loses stability and bifurcation to cellular steady-state interfaces takes place in virtue of the nonlinear terms M_i in (2.11). We confine ourselves to stationary solutions of (2.11), $\dot{\varepsilon}_i=0$. Suppose that for $v=v_c$, $a_n=0$ is the first eigenvalue going through zero, and $a_i<0$ for $i\neq n$. Then the nth equation in (2.11) has a vanishing linear part, i.e., it is degenerate. According to the implicit function theorem, the nondegenerate equation system (2.11) with $i\neq n$ can be solved uniquely with respect to the ε_i, $i\neq n$, i.e., $\varepsilon_i=\varepsilon_i(\varepsilon_n)$. Substituting this expression into the degenerate equation with $i=n$ yields a single algebraic equation for the stationary amplitude ε_n:

$$B(\varepsilon_n,v):=M_n(\varepsilon(\varepsilon_n))=0 \tag{2.12a}$$

with $B(0,v_c)=0$ and $\partial B(0,v_c)/\partial\varepsilon_n=0$. In virtue of the symmetry of the equations of motion (2.1)–(2.3) with respect to reflections at the axis $\xi=b/2$ and the nonflux boundary conditions (2.4), B is an odd function of ε_n, i.e., $B(-\varepsilon_n,v)=-B(\varepsilon_n,v)$, so that (2.12a) takes the form

$$B(x,v)=xh(x^2,v)=0 \tag{2.12b}$$

with $x\equiv\varepsilon_n$, where $h(x^2,v)$ is a smooth function with $h(0,v_c)=0$. If n is odd, (2.12b) simply is a result of the reflection symmetry of the equations of motion. For n even, however, the special form of B is a nontrivial consequence of the nonflux boundary conditions.[21–23] We do not give a proof here but confine ourselves to a simple plausibilty argument. Since the equations of motion (2.1)–(2.3) are invariant under a reflection at the axis $\xi=b/2$, then with $s(\xi,t)$, $s(b-\xi,t)$ also represents an interface. Suppose now that s in (2.9) consists only of a single mode $s=\varepsilon_n\cos(n\sqrt{u}\,k_0\xi)$. If n is odd, then

$$\begin{aligned}s(b-\xi,t)&=\varepsilon_n\cos[n\sqrt{u}\,k_0(b-\xi)]\\&=-\varepsilon_n\cos(n\sqrt{u}\,k_0\xi)=-s(\xi,t)\end{aligned}$$

is also an interface pertaining to a solution of (2.1)–(2.5). Consequently, together with ε_n, $-\varepsilon_n$ is also a solution of (2.12a). If n is even, we note that at $\xi=b/2$ the interface

$s=\varepsilon_n\cos(n\sqrt{u}\,k_0\xi)$ also satisfies the condition $s_{\xi}=0$. In this case we can consider the interface in the intervals $[0,b/2]$ and $[b/2,b]$. If $n/2$ is odd, we can apply the above argument to each of the intervals $[0,b/2]$ and $[b/2,b]$ with the result that $-\varepsilon_n$ is a solution of (2.12a). If, on the other hand, $n/2$ is even, we divide the interval $[0,b]$ into $[0,b/4],\ldots,[3b/4,b]$ and consider s in each of these intervals, and so forth. Hence, if ε_n is a solution of $B=0$, $-\varepsilon_n$ is also a solution. By explicit calculation (cf. the Appendix) one can show that all even derivatives of B with respect to x vanish at $x=0$, whence (2.12b) follows.

As we shall see in the Sec. II C, it is possible that, for $v=v_c$, two neighboring eigenvalues a_n and a_{n+1} can vanish simultaneously. Then, the system (2.11) possesses two degenerate equations, viz., the equations with $i=n$ and $i=n+1$. Solving the remaining nondegenerate equation system (2.11), $i\neq n$, $n+1$, for ε_n and ε_{n+1} to yield $\varepsilon_i=\varepsilon_i(\varepsilon_n,\varepsilon_{n+1})$ and substituting these expressions into the two degenerate equations with $i=n$, $n+1$, gives two coupled equations:

$$B^{(1)}(\varepsilon_n,\varepsilon_{n+1},v)=0\,,\qquad B^{(2)}(\varepsilon_n,\varepsilon_{n+1},v)=0\,, \tag{2.13a}$$

with $B^{(i)}(0,0,v_c)=0$ and

$$\partial B^{(1)}(0,0,v_c)/\partial\varepsilon_n=\partial B^{(2)}(0,0,v_c)/\partial\varepsilon_{n+1}=0\,.$$

It has been shown by Dangelmayr and Armbruster[22,23] that any bifurcation problem of the type (2.13a) for two coupled stationary modes with nonflux boundary conditions possesses the form

$$B^{(1)}(x,y,v)=xa(x^2,y^2,v)+x^ny^nb(x^2,y^2,v)=0\,,$$
$$B^{(2)}(x,y,v)=yc(x^2,y^2,v)+x^{n+1}y^{n-1}d(x^2,y^2,v)=0\,, \tag{2.13b}$$

where $x\equiv\varepsilon_n$, $y\equiv\varepsilon_{n+1}$, $n\geqq 1$, and a,b,c,d are smooth functions. The bifurcation behavior depends on the wave numbers n of the two unstable modes. The functions $B,B^{(1)},B^{(2)}$ depend also on the system parameters u,k_0 which will be taken into account in Sec. III.

C. Linear stability analysis

According to (2.11), the planar interface loses stability as v increases if one or more eigenvalues a_i of the linearized system $\dot{\varepsilon}_i=a_i\varepsilon_i=0$ go through zero from negative values. We have

$$a_n=(v-1-n^2k_0^2)\left[\frac{v}{2}+\left[\frac{v^2}{4}+un^2k_0^2\right]^{1/2}\right]-v^2 \tag{2.14}$$

from which we obtain v_c by setting $a_n=0$ and solving for v. Thus, considering nk_0 as a continuous variable k for a moment, instability at $v=v_c$ sets in if, for a given u, the surface

$$a(k,v,u)=(v-1-k^2)\left[\frac{v}{2}+\left[\frac{v^2}{4}+uk^2\right]^{1/2}\right]-v^2$$

in (k,v,a) space intersects the (k,v) plane. Such intersection occurs in a convex contour $C(u)$ when $u\geqq 27$ (Fig. 2) and the mode $\cos(m\sqrt{u}\,k_0\xi)$ becomes unstable if the line $k=mk_0$ parallel to the v axis intersects $C(u)$. Then, if the interface velocity v increases, the mode pertaining to the lowest value of v at the intersection points is the first one that becomes unstable. We call this the critical mode. From Fig. 2 one infers that the system restabilizes for a sufficiently high velocity. Because we are only interested in the onset of instability, we have to consider only the lower part of the contour $C(u)$.

If u increases, the contour $C(u)$ expands so that criticality of a mode depends on the values of both k_0 and u. We show that the (k_0,u) plane can be divided into disjoint regions R_n, $n=1,2,3,\ldots$, such that for any choice of (k_0,u) within R_n, precisely the nth mode is critical (Fig. 3). Suppose (k_0,u) is located in R_n. Then the nth mode is critical. If we now vary (k_0,u) and cross the boundary of R_n, the mode number n ceases to be critical and there are two ways for this to happen: (a) If $nk_0=k_-$ (or k_+) where

$$k_{\mp}^2=\{2u-27\mp[u(u-27)]^{1/2}\}/27$$

and $k_{\mp}$ are the abscissas of the left and right vertical tangents to $C(u)$ (Fig. 2), and k_0 is decreased (or increased), then a_n does not vanish and the $(n+1)$-th mode becomes critical (or no critical mode is present) [Fig. 4(a)]; (b) If two modes n and $n+1$ are simultaneously critical [Fig. 4(b)], a decrease or increase of k_0 results in a situation where only the $(n+1)$-th or the nth mode, respectively, is critical. Since $C(u)$ is convex, at most two neighboring modes can simultaneously be critical. The condition $nk_0=k_{\mp}$ yields curves W_n in the (k_0,u) plane which are given by

$$u=27(1+n^2k_0^2)^2/(4n^2k_0^2). \tag{2.15}$$

Eliminating v from $a_n=a_{n+1}=0$ yields a set of curves Z_n in the (k_0,u) plane (Fig. 5). The curves W_n and Z_n intersect in various points. The reason for this is that these curves describe bifurcation phenomena at destabilization

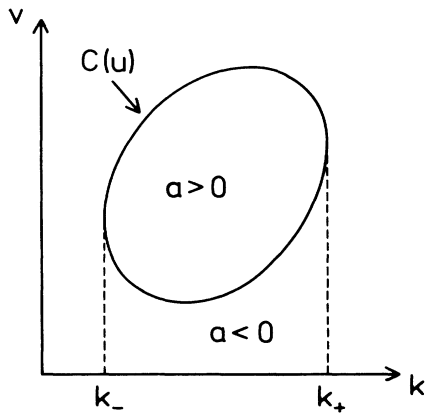

FIG. 2. Critical values of the interface velocity v as a function of the rescaled wave number k.

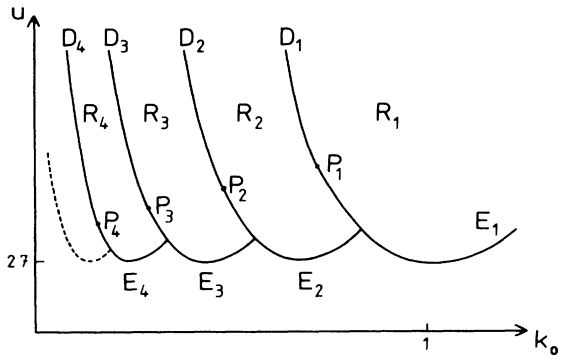

FIG. 3. Division of the (k_0,u) plane indicating the critical modes. For (k_0,u) lying in region R_n, $n\in\mathbb{N}$, the mode number n becomes unstable first for increasing interface velocity v and thus determines the wavelength of the emerging cellular interface.

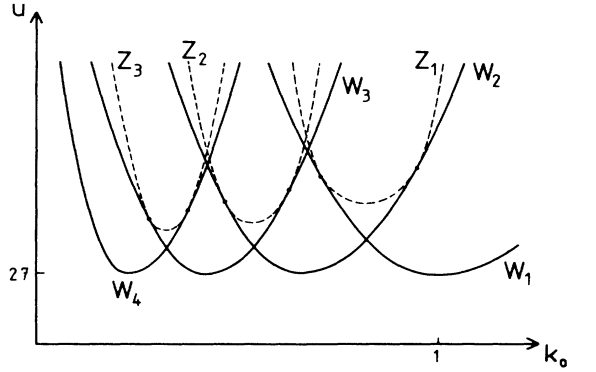

FIG. 5. Curves W_n and Z_n resulting from the conditions $nk_0=k_\pm$ and $a_n=a_{n+1}$ at $v=v_c$, respectively. Parts of these curves constitute the boundaries of the regions R_n in Fig. 3.

and at restabilization. For example, for fixed u we have two different values of k_0 for which two neighboring eigenvalues a_n and a_{n+1} vanish simultaneously for some v. But for one of these values of k_0 the vanishing of the eigenvalues occurs at restabilization and not at destabilization and, therefore, is not relevant for the onset of instability. Since $C(u)$ is inclined to the right, the smaller k_0 value belongs to destabilization. With similar arguments one can sort out those parts of the curves W_n and Z_n, E_n and D_n, respectively, which are meaningful for the onset of instability, and finally obtain Fig. 3. Here $P_n=(k_n^*,u_n^*)$ is a point of contact of the curves W_n and Z_n (cf. the Appendix). E_n is the part of W_n with $k_0\geqq k_n^*$, and D_n is the part of Z_n with $k_0\leqq k_n^*$. Hence, if (k_0,u) lies in R_n or on E_n the nth mode is critical; if (k_0,u) lies on D_n the nth and $(n+1)$-th modes are simultaneously critical. Outside the union of all R_n the planar interface remains stable for all v.

III. NONLINEAR BIFURCATION ANALYSIS

In this section we present a fully nonlinear analysis of the bifurcation equations (2.12) and (2.13) near the onset of instability. We use the theory of imperfect bifurcations[18,19] to determine and to classify the generic bifurcation processes that can occur in the solidification model and analyze the effects of imperfections and parameter variations on the bifurcation diagrams. In order to make the exposition self-contained, we summarize first the basic concepts and results of imperfect bifurcation theory and then apply them to the problem of cellular interface bifurcations.

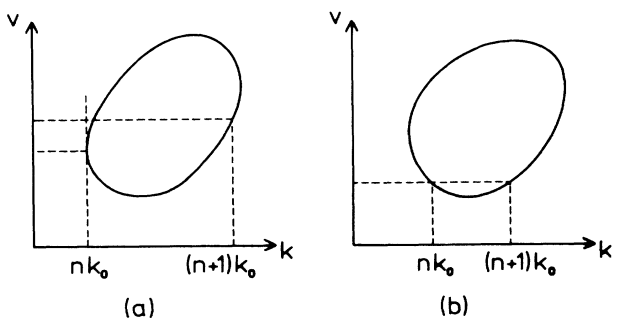

FIG. 4. Borderline cases for the change in being the critical mode between modes number n and $n+1$. (a) $nk_0=k_-$, (b) double-zero eigenvalue.

A. Imperfect bifurcation theory

A general "bifurcation problem"[18,24] g consists of finding the solutions $x=x(\lambda)$ of a system of equations

$$g(x,\lambda)=0 \tag{3.1}$$

with $g(0,0)=g_x(0,0)=0$, where $g=(g_1,g_2,\ldots,g_n)$ is a smooth function, $x=(x_1,x_2,\ldots,x_n)$ are state variables, and λ is a distinguished bifurcation parameter representing the control variable in a physical experiment. It is assumed that (3.1) is the equation system for the amplitudes x of the solution of a given nonlinear evolution equation, obtained by a Lyapunov-Schmidt reduction. The point $(x,\lambda)=(0,0)$ is a bifurcation point or a singularity of g, and the solutions (x,λ) of (3.1) constitute the bifurcation diagram. In the solidification problem, the bifurcation equations (3.1) are identical with (2.12) in the single-mode case with $x_1=x=\varepsilon_n$, $g=B$, and with (2.13) in the double-mode case with $x_1=\varepsilon_n$, $x_2=\varepsilon_{n+1}$, $g_1=B^{(1)}$, $g_2=B^{(2)}$, respectively, and $\lambda=v-v_c$ in both cases.

Two functions $g(x,\lambda)$ and $g'(x,\lambda)$ are called equivalent or "qualitatively similar" if there exist smooth local coordinate changes $x\to X(x,\lambda)$ and $\lambda\to\Lambda(\lambda)$ with $\det X_x(0,0)\neq 0$ and $\Lambda_\lambda(0)>0$ so that

$$g(x,\lambda)=T(x,\lambda)g'(X(x,\lambda),\Lambda(\lambda))\,, \tag{3.2}$$

where T is a square matrix with $\det T(0,0)>0$. Since Λ may not depend on x, the control parameter λ influences x, but not conversely. Since T is invertible, two equivalent bifurcation problems possess qualitatively the same solution set. The effects of perturbations in a system are incorporated into the bifurcation problem (3.1) by

the unfolding of g. A k-parameter function $G(x,\lambda,\alpha)$, with $G(x,\lambda,0)=g(x,\lambda)$ is called an unfolding of g with unfolding or imperfection parameters $\alpha=(\alpha_1,\alpha_2,\ldots,\alpha_k)$. If for any sufficiently small perturbation $\varepsilon p(x,\lambda,\varepsilon)$ there exists an α so that the perturbed bifurcation problem $g+\varepsilon p$ is equivalent [in the sense of (3.2)] to $G(x,\lambda,\alpha)$ and if k is the minimum number of unfolding parameters needed to describe the perturbation, then $G(x,\lambda,\alpha)$ is called a stable or universal unfolding of g, and k is called the codimension of g. The codimension is a measure for the degree of complexity of the bifurcation problem. We have the following theorem:[18,19] If g has finite codimension, then there exists a polynomial $g'=N(x,\lambda)$, called a normal form, which is equivalent to g, and a universal unfolding $G'=F(x,\lambda,\alpha)$ of N which is also a polynomial. (Here the new variables X and Λ are denoted again by x and λ.) By varying α in $F(x,\lambda,\alpha)=0$ one obtains a finite number of qualitatively different, perturbed, or unfolded bifurcation diagrams. The α-parameter space can be divided into a finite number of regions such that for any two parameter values lying within the same region the corresponding bifurcation problems are equivalent and structurally stable. Crossing the boundaries separating these regions produces new qualitatively different diagrams.

Changes in the stability properties of a solution x of $F=0$ follow by considering x as equilibrium solution of the system $\dot{x}=F(x,\lambda,\alpha)$. The signs of the real parts of the eigenvalues of the Jacobian of F evaluated at x determine the stability properties of the bifurcating solution branches of $F=0$. In order that bifurcation occurs in (3.1) and g is equivalent to a normal form, g must satisfy certain defining (or degeneracy) conditions which express the vanishing of some of its first derivatives and certain nondegeneracy conditions which relate to the nonvanishing of some next higher derivatives. With these techniques it is possible to classify bifurcation problems by their codimension, i.e., to give a list of all possible bifurcation diagrams.

The imperfect bifurcation theory outlined above can be generalized to problems with symmetry.[18,19] g is called to be a bifurcation problem with symmetry group Γ if g is Γ covariant, i.e., if $g(\gamma x,\lambda)=\gamma g(x,\lambda)$ for all $\gamma\in\Gamma$. g and g' are Γ equivalent if (3.2) holds with the symmetry conditions $X(\gamma x,\lambda)=\gamma X(x,\lambda)$ and $T(\gamma x,\lambda)=\gamma T(x,\lambda)\gamma^{-1}$. The notions of Γ-covariant unfolding, Γ codimension, etc., are defined in an analogous way.

The following example is instructive. Let $x\in\mathbb{R}$ and let $\Gamma=Z(2)$ be the reflection group so that $g(-x,\lambda)=-g(x,\lambda)$. Suppose that g satisfies the defining condition $g_{xxx}=0$ and the nondegeneracy condition $g_\lambda g_{xxxxx}>0$ at $(x,\lambda)=(0,0)$. Then the bifurcation problem $g(x,\lambda)=0$ is $Z(2)$-equivalent to the $Z(2)$-codimension-1 normal-form problem $g'=N=x^5+\lambda x=0$ with the $Z(2)$-universal unfolding $F=x^5+2\alpha x^3+\lambda x=0$. The solution set of $F=0$ consists of the qualitatively different bifurcation diagrams shown in Fig. 9 below for various values of α. (In Fig. 9 only the solutions with $x\geqq 0$ are shown.)

As has been mentioned at the end of Sec. II B, the $B,B^{(i)}$ depend on the system parameters u,k_0. Therefore, the left-hand sides of the defining and nondegeneracy conditions [of the type $g_x(0,0)=0,g_{x\lambda}(0,0)=0,g_{xxx}(0,0)\neq 0$] are now functions of k_0 and u. Hence, for each normal form there exists a set of points (k_{0c},u_c) in the (k_0,u) plane for which these conditions are satisfied and for which bifurcations can occur. Thus, a $Z(2)$-symmetry-preserving perturbation of the system (there are others, naturally) consists of a deviation of (k_0,u) from (k_{0c},u_c). As we shall see in the following, such a perturbation can be described by the unfolded normal forms of the bifurcation problems through an identification of $k_{0c}-k_0$ and u_c-u with unfolding parameters α.

B. Single-mode bifurcation

In this section we determine the qualitatively different bifurcation diagrams which describe the various transitions between planar and cellular interfaces if a single mode becomes unstable at $v=v_c$. In Sec. II B we have shown that the bifurcation equation (2.12a) has the form

$$B(x,v)=xh(x^2,v),\quad h(0,v_c)=0\,, \tag{3.3}$$

where $x=\varepsilon_n$ is the amplitude of the mode and bifurcation occurs at $x=0$ for $\lambda=v-v_c=0$. Reflection-symmetric bifurcation problems of the form (3.3) have been classified by Golubitsky and Langford[25,19] in the context of degenerate Hopf bifurcations. The derivatives of B at $x=0$, $v=v_c$ which occur in the various defining and nondegeneracy conditions can be calculated explicitly as functions of the coefficients $a^{(m)}_{m_1,m_2,\ldots,m_j}$, i.e., as functions of the system parameters k_0 and u (cf. the Appendix). In what follows all derivatives of B are taken at $x=0$ and at $v=v_c$ unless stated otherwise.

In the list of normal forms given in Ref. 25 there are two defining conditions, viz., in the present case, $B_{xv}=0$ and $B_{xxx}=0$ at $x=0$, $v=v_c$, whose validity determines the type of the normal form describing the bifurcation.

TABLE I. Unfolded normal forms for single-mode bifurcations occurring in the solidification model (2.1)–(2.5).

Unfolded normal form	Location of (k_0,u)	Figure
(1) $x^3-\lambda x$	Below K_n^-, $n\geqq 1$	7(a)
(2) $x^3+\lambda x$	Above K_n^-, $n\leqq 3$	7(b)
(3) $x^3+(\lambda^2+\alpha)x$	On E_n, left of T_n, $n\geqq 1$	8 (top)
(4) $x^3-(\lambda^2+\alpha)x$	On E_n, right of T_n, $n\leqq 3$	8 (bottom)
(5) $x^5+2\alpha x^3-\lambda x$	On K_n^-, $n\leqq 3$	9
(6) $x^5-2\mu\lambda x^3+(\lambda^2-\beta\lambda+\alpha)x$	At T_n, $n\leqq 2$	10

Therefore, we determine first the set of parameters (k_0,u) for which these conditions are satisfied: (a) We have $B_{xv}=\partial a_n/\partial v$. $a_n=0$ and $B_{xv}=0$ give $v_c=3r$ and $u=27r^2/[4(r-1)]$ where $r:=1+n^2k_0^2$, describing the curve W_n of Fig. 5. (b) To analyze the second condition, $B_{xxx}=0$, we note that

$$B_{xxx}=6(a_{2n}^{(2n)}a_{-n,n,n}^{(n)}-a_{-n,2n}^{(n)}a_{n,n}^{(2n)})/a_{2n}\ . \tag{3.4}$$

Eliminating u from $B_{xxx}=0$ and $a_n=0$ yields the equation

$$v_c^3+12rv_c^2-r(20r^2-5r+12)v_c+2r^3(4r+3)=0\ . \tag{3.5}$$

From $a_n=0$ one obtains

$$u=v_c^3r/[(r-1)(v_c-r)^2]\ . \tag{3.6}$$

Eliminating v from (3.5) and (3.6) gives the curve K_n in the (k_0,u) plane (Fig. 6) which has a contact with W_n at the point $T_n=(\hat{k}_n,\hat{u})$ where

$$\hat{k}_n=\frac{1}{n^2}(\tfrac{1}{2}+\tfrac{9}{26}\sqrt{13})\cong 1.748/n^2\ ,$$

$$\hat{u}=\tfrac{243}{884}(52+15/\sqrt{13})\cong 29.16\ .$$

An argument similar to that used in Sec. II C shows that only the branch K_n^- of K_n to the left of T_n describes destabilization of the planar interface while the right branch corresponds to restabilization, and only for $n\leqq 3$ is K_n^- located inside the region R_n. Furthermore, T_n lies inside R_n only for $n=1$ and $n=2$. With these results we can determine all bifurcation diagrams. The corresponding normal forms are given in Table I. For (k_0,u) in R_n we find the following.

(i) If (k_0,u) lies neither on K_n^- nor on E_n, then $B_{xv}\neq 0$ and $B_{xxx}\neq 0$. Hence, from Ref. 25 we obtain the normal form (1) of Table I, viz., $N=x^3-\lambda x$ if $B_{xv}B_{xxx}<0$ and $N=x^3+\lambda x$ if $B_{xv}B_{xxx}>0$. It turns out that B_{xv} is always positive if (k_0,u) is above E_n and that B_{xxx} is positive if (k_0,u) is above K_n^- and negative below. Therefore, in regions c and d of Fig. 6 we encounter a subcritical bifurcation, and in region e a supercritical one. These bifurcations have $Z(2)$ codimension-0 and are not altered by small $Z(2)$-preserving perturbations. The corresponding diagrams are shown in Fig. 7. The stability symbols "s" and "u" mean stable and unstable and in virtue of the $Z(2)$ symmetry of the system only the branches with $x\geqq 0$ are shown.

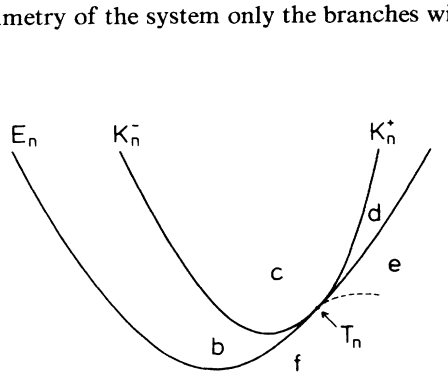

FIG. 6. Location of the curves K_n in the (k_0,u) plane. On K_n we have $B_{xxx}(0,v_c)=0$.

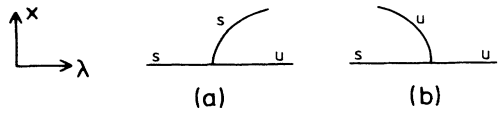

FIG. 7. Bifurcation diagrams for the normal forms (a) $x^3-\lambda x$ and (b) $x^3+\lambda x$. s means stable, u unstable.

(ii) On the curve E_n, excluding T_n, we have $B_{xv}=0$ and $B_{xxx}\neq 0$. Then the corresponding normal form is determined by the signs of B_{xxx} and B_{xvv}. Since $B_{xvv}=\partial^2 a_n/\partial v^2=-\frac{3}{8}$ for (k_0,u) on E_n, the bifurcations are determined by the normal form (3) of Table I on the part of E_n to the left of T_n (where $B_{xxx}<0$) and by normal form (4) on the part to the right of T_n (where $B_{xxx}>0$). These are $Z(2)$-codimension-1 bifurcations with diagrams shown in Fig. 8. In particular, for (k_0,u) on E_n the bifurcation behavior of the system is described by Fig. 8 (top) (b) provided that (k_0,u) lies to the left of T_n. If the system is perturbed by a small $Z(2)$-symmetry-preserving perturbation, it is described by the universal unfolding of (3), viz., by the diagrams of Fig. 8 (top) (a) and (c). The most obvious symmetry-preserving perturbations are deviations of (k_0,u) from their values taken on E_n. As we have seen, (k_0,u) lies on E_n if $nk_0=k_-$ (or $nk_0=k_+$) in Fig. 2. When we now shift k_0 slightly to the left (or decrease u), then the nth mode does not become unstable at all. This situation is described by the bifurcation diagram shown in Fig. 8 (top) (c). Shifting k_0 to the right has the effect that, with increasing v, the nth mode restabilizes shortly after destabilization. This gives Fig. 8 (top) (a). Thus, we see that perturbations described by the unfolding parameter α can in fact be identified with deviations of (k_0,u) from the values taken on the curve E_n.

(iii) The normal form which corresponds to a point

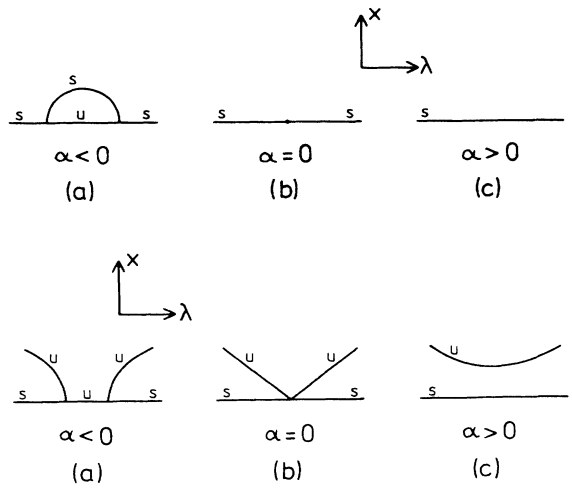

FIG. 8. (Top): diagrams for normal form (3) of Table I. (a) $\alpha<0$, (b) $\alpha=0$, (c) $\alpha>0$. Bottom: diagrams for normal form (4) of Table I. (a) $\alpha<0$, (b) $\alpha=0$, (c) $\alpha>0$.

(k_0,u) on K_n^-, excluding T_n, depends on the sign of B_{xxxxx}. A numerical analysis shows that B_{xxxxx} is negative on K_n^- so that the bifurcation is described by the normal form (5) of Table I, viz., by $N=x^5-\lambda x$ with unfolding $F=x^5+2\alpha x^3-\lambda x$. The bifurcation diagrams are shown in Fig. 9. Here, for the first time a hysteresis bifurcation behavior occurs and, since it is a codimension-1 phenomenon, it should be frequently observable in solidification experiments.

(iv) For (k_0,u) on the point T_n the equations $B_{xv}=0$ and $B_{xxx}=0$ hold simultaneously and the associated nondegeneracy conditions are $B_{xvv}\neq 0$, $B_{xxxxx}\neq 0$, and $\mu^2\varepsilon\neq 1$, where $\varepsilon=\mathrm{sgn}(B_{xvv}B_{xxxxx})$ and $\mu=B_{xxxv}/(|B_{xvvv}B_{xxxxx}|)^{1/2}$. Since B_{xvv} and B_{xxxxx} are both negative at T_n, we have $\varepsilon=+1$ and a numerical calculation yields $\mu=-0.2209$ whence $\mu^2\varepsilon\neq 1$. Therefore, the normal form describing the situation where (k_0,u) lies on the point T_n is $N=x^5-2\mu\lambda x^3+\lambda^2 x$ with universal unfolding $F=x^5-2\mu\lambda x^3+(\lambda^2-\beta\lambda+\alpha)x$ and unfolding parameters α and β. The bifurcation diagrams derived from $F=0$ are shown in Fig. 10 for various ranges of values of α and β. In addition to hysteresis, there appear new bifurcation phenomena, viz., the mushroom bifurcation [Fig. 10(d)] and the formation of an island [Fig. 10(e)], i.e., of a stable cellular interface which is not connected to the planar interface and which occurs without any apparent instability present in the planar solidification front. Such stable islands are also familiar from bifurcation phenomena in chemical reactions and optical bistability.[26] Here we can again identify the unfolding parameters with deviations of (k_0,u) from T_n. If (k_0,u) lies in region $\mathscr{b}$ of Fig. 6 near T_n, the system undergoes a supercritical bifurcation since B_{xxx} is negative there and restabilizes thereafter subcritically since $B_{xv}<0$ at restabilization, a result described by Fig. 10(b). If (k_0,u) crosses the curve K_n from region $\mathscr{b}$ to region c, bifurcation at destabilization changes from supercritical to subcritical, cf. Fig. 10(c). When (k_0,u) is moved from region c to region $\mathscr{d}$, the bifurcation at restabilization changes from subcritical to supercritical and thus produces the mushroom diagram of Fig. 10(d). Passing from region $\mathscr{d}$ to region e, the primary bifurcations disappear, i.e., the mushroom's head disconnects from its basis and we are left with the island of Fig. 10(e). When (k_0,u) crosses E_n from region $\mathscr{b}$ to region $\mathscr{f}$, the primary bifurcations disappear too, so that in region $\mathscr{f}$ we are left with the diagram of Fig. 10(f). Within the framework of the one-sided solidification model these are all the single-mode bifurcations that can occur.

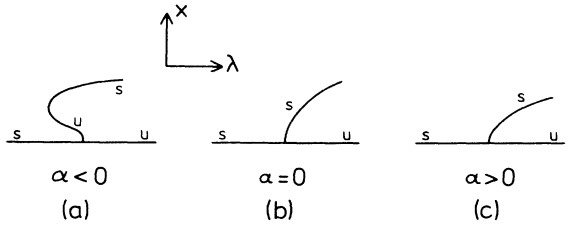

FIG. 9. Diagrams for normal form (5) of Table I. (a) $\alpha<0$, (b) $\alpha=0$, (c) $\alpha>0$.

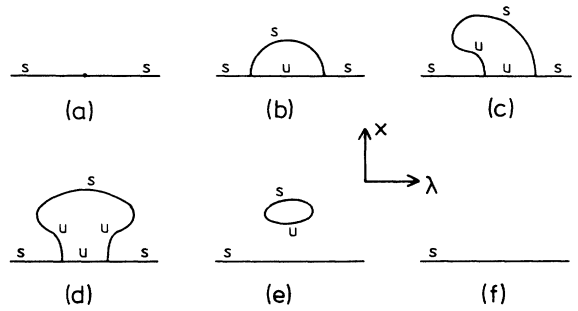

FIG. 10. Diagrams for normal form (6) of Table I. (a) $\alpha=\beta=0$, (b)–(f) all qualitatively different diagrams for various values $a\neq 0$, $\beta\neq 0$.

C. Two-mode interactions

The objective of this section is to discuss the simultaneous bifurcation and subsequent interaction of two critical modes when the planar interface loses stability. According to Sec. IIC this occurs for two neighboring modes $\varepsilon_n\cos(\sqrt{u}\,nk_0\xi)$ and $\varepsilon_{n+1}\cos[\sqrt{u}\,(n+1)k_0\xi]$ when (k_0,u) is located on the curve D_n in Fig. 3. A classification up to codimension-2 and an unfolding theory of bifurcation equations with such double-zero eigenvalues and nonflux boundary conditions has been developed by Armbruster and Dangelmayr.[22,23] In the present case of two neighboring critical modes their bifurcation equations take the form

$$\begin{aligned} B^{(1)}(x,y,v)&=xa(x^2,y^2,v)+x^n y^n b(x^2,y^2,v)=0\,,\\ B^{(2)}(x,y,v)&=yc(x^2,y^2,v)+x^{n+1}y^{n-1}d(x^2,y^2,v)\\ &=0\,, \end{aligned} \tag{3.7}$$

where $x\equiv\varepsilon_n$, $y\equiv\varepsilon_{n+1}$, and a,b,c,d are smooth functions and $n\geq 1$. From (3.7) it follows that the bifurcation behavior depends on the wave numbers n and $(n+1)$ of the two unstable modes.

The solutions of (3.7) can be divided into different branches. The trivial solution $x=y=0$ describes always the planar interface. In the case $n=1$, a pure-mode solution S_y with amplitude y follows from $x=0$ and $c=0$ while a mixed-mode solution S_m with amplitudes $x\neq 0, y\neq 0$ is given by the solution of $a+yb=0$ and $yc+x^2d=0$. In the case $n\geq 2$ we have the pure-mode solution S_x with amplitude x from $y=0$ and $a=0$, the pure-mode branch S_y follows from $x=0$ and $c=0$, and the mixed-mode solution S_m is given by $a+x^{n-1}y^n b=0$ and $c+x^{n+1}y^{n-2}d=0$. In both cases the S_x and S_y branches bifurcate from the planar interface $(x=y=0)$, i.e., at a primary bifurcation point. The S_m branches bifurcate in general at secondary bifurcation points, i.e., off the trivial solution, and connect the pure-mode branches, cf. Figs. 14–16 below. The mixed modes give rise to spatial beats and to mode jumping. Obviously, each pure-mode bifurcation individually has a $Z(2)$ symmetry because for $x=0$ or $y=0$ the second terms in (3.7) both vanish. Thus the generic primary bifurcation is the pitch-

fork. However, the branches S_m do not possess a $Z(2)\times Z(2)$ symmetry in virtue of the terms b and d, because one of the second terms in (3.7) is even in x and y and the other is odd.

The normal forms and diagrams describing the two-mode bifurcations of the solidifying interface are derived in essentially the same way as in Sec. III B. The derivatives of $B^{(1)}$ and $B^{(2)}$ at $x=y=0, v=v_c$ needed for the defining and nondegeneracy conditions are calculated as in the case of single-mode criticality. The conditions which have to be satisfied must again be divided into two classes, viz., $n=1$ and $n\geqq 2$ in Eq. (3.7).

(1) In the case $n=1$, there are five codimension-2 normal forms[22] with defining conditions

$$B^{(1)}_{xv}=0,\quad B^{(1)}_{xy}=0\ ,\qquad B^{(2)}_{yyy}=0,\quad B^{(2)}_{yv}=0,\quad B^{(2)}_{xx}=0 \tag{3.8}$$

(taken at $x=y=0, v=v_c$). We have $B^{(1)}_{xv}=\partial a_1/\partial v=0$, which leads, together with $a_1=0$, to the curve E_1 that intersects D_1 at the point P_1 of Fig. 3. Furthermore, we have $B^{(1)}_{xy}=a^{(1)}_{-1,2}$ which, together with (3.6), yields

$$B^{(1)}_{xy}=[3v_c^2k_0^2(1+4k_0^2)]/[2(v_c-1-4k_0^2)^2]\ ,$$

a quantity which is always positive. $B^{(2)}_{yyy}$ is given by the right-hand side of Eq. (3.4) with n replaced by 2. Hence $B^{(2)}_{yyy}=0$ leads to the curve K_2^- and to the equation (3.5) with r replaced by $1+4k_0^2$. Substituting for v_c its value on D_1 (cf. the Appendix) gives a cubic equation for k_0^2 whose zeros are off the curve D_1. Therefore, $B^{(2)}_{yyy}>0$ on D_1. By similar arguments one finds that $B^{(2)}_{yv}>0$ and $B^{(2)}_{xx}<0$ on D_1 and $B^{(1)}_{xvv}<0$ at P_1. Consequently, among the five codimension-2 normal forms listed in Ref. 22, only the one with $B^{(1)}_{xv}=0$ occurs in the present case and the bifurcation for $(k_0,u)=P_1$ is described by the unfolded normal form

$$-x(y+\lambda^2+\alpha+\beta\lambda)=0\ ,\qquad x^2+y(y^2+\lambda)=0\ , \tag{3.9}$$

with unfolding parameters α and β.

The solutions of (3.9) are bifurcation diagrams in (λ,x,y) space. In Fig. 11 projections onto the (λ,y) plane of the topologically distinct bifurcation diagrams for various α and β are shown. The pure-mode solution S_y is given by $x=0, y^2=-\lambda$, S_m is the mixed-mode solution with $x\neq 0$, $y\neq 0$. It possesses a branch with $x>0$ and one with $x<0$. The $(+,-)$ signs on the solution branches are those of the real parts of the eigenvalues of the Jacobian of (3.9) and indicate the stability of the branches, [$(-,-)$ means stable, all others unstable]. Figure 11(b) shows a mixed-mode solution branch which bifurcates supercritically from the planar interface with stability symbol $(-,-)$ and connects S_y subcritically with $(+,+)$. This implies that at the point TB a tertiary bifurcation occurs, which is here a Hopf bifurcation to time-periodic solutions (a pair of complex eigenvalues crosses the imaginary axis). This bifurcation describes a standing wave with a spatial modulation of the mode $\cos(\sqrt{u}\,k_0\xi)$ by the mode $\cos(2\sqrt{u}\,k_0\xi)$. We observe that every bifurcation is locally of pitchfork type.

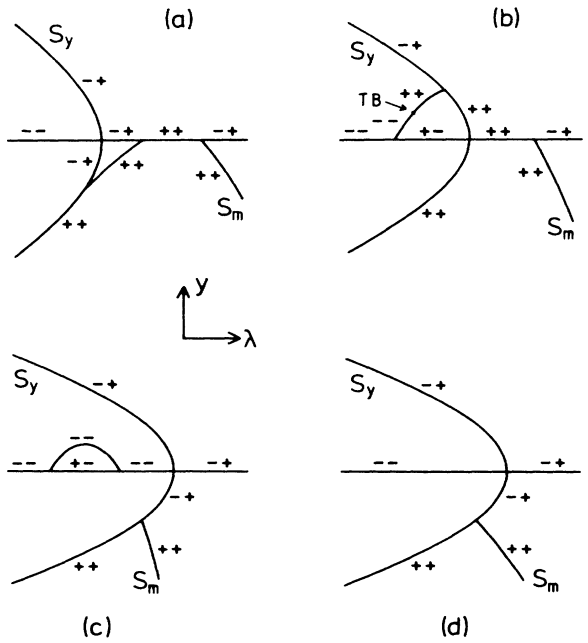

FIG. 11. Diagrams for the unfolded normal form (3.9) for $(k_0,u)=P_1$ and $n=1$. The solutions are projected onto the (λ,y) plane. The $(+,-)$ signs indicate stability, where $(-,-)$ means stable, all others unstable. (a)–(d) show the four qualitatively different diagrams for various values of the unfolding parameters α and β. In (b) we have at the point TB a tertiary bifurcation to time-periodic states.

In analogy to the case of single-mode bifurcation, the four types of bifurcation, shown in Fig. 11, can be obtained by varying (k_0,u) around the point P_1. If (k_0,u) is on D_1 near P_1, the two modes become simultaneously unstable and, as v increases beyond v_c, the first mode restabilizes shortly thereafter [Fig. 12(b)]. If k_0 is slightly decreased, so that (k_0,u) moves into region a of Fig. 12(a), the second mode becomes unstable first and this is followed by an instability of the first mode which restabilizes thereafter [Fig. 12(c)]. Since the diagrams of Fig. 11 are characterized uniquely by the sequence of primary bifurcations of S_y and S_m, we arrive at the diagram of Fig. 11(a). By similar arguments we establish correspondences between the regions b, c, and d of Fig. 12(a) and the diagrams (b), (c), and (d) in Fig. 11, respectively. If (k_0,u) is located on D_1, excluding P_1, the bifurcation is described by a codimension-1 normal form and by the diagrams of Fig. 13.

(2) In the case $n\geqq 2$ there are seven codimension-2 normal forms[22] with defining conditions

$$B^{(1)}_{xxx}=0,\quad B^{(1)}_{xv}=0,\quad B^{(2)}_{yyy}=0,\quad B^{(2)}_{yv}=0\ , \tag{3.10}$$

and three additional conditions involving some vanishing determinants with mixed derivatives with respect to x and y. An analysis similar to that for the case $n=1$ shows that only the condition $B^{(1)}_{xv}=0$ can be satisfied for (k_0,u) at the point P_n in Fig. 3. Therefore, we infer from Ref. 22 that at P_n the unfolded normal form is

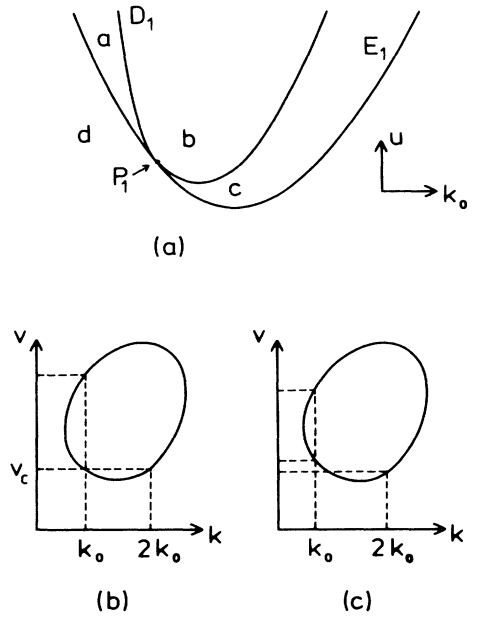

FIG. 12. (a) The curves W_1 and Z_1 near the point P_1 in the (k_0,u) plane. (b) Situation in the (k,v) plane corresponding to (k_0,u) lying on the curve D_1. (c) Situation corresponding to (k_0,u) lying in region α of (a).

$$x(-x^2-y^2-\lambda^2+\mu_1 x^{n-1}y^n+\alpha)=0\,,$$
$$y(\kappa x^2+\varepsilon y^2+\lambda+\mu_2 x^{n+1}y^{n-2}+\beta)=0\,, \tag{3.11}$$

with unfolding parameters α and β. Here $\varepsilon=+1$ and $\mu_i<0$ for $n=2$, $\mu_i\neq 0$ for $n=3$ and $\varepsilon=-1$ for $n\geq 3$, and κ is defined by

$$\kappa=B^{(2)}_{xxy}\,|\,B^{(1)}_{xyy}\,|\,/\,|\,B^{(1)}_{xxx}B^{(2)}_{yyy}\,|$$

with the derivatives taken at $x=y=0, v=v_c$. The μ_i are modal unfolding parameters which are characterized by the fact that they parametrize the largest family of perturbations of N such that no two perturbations in this family are equivalent. The bifurcation diagrams described by (3.11) are shown in Figs. 14, 15, and 16 for the cases $n=2$, $n=3$, and $n\geq 4$, respectively. Again, there is the familiar correspondence between the perturbed diagrams and the (k_0,u) values varying around P_n. The pure-mode solutions S_x with $y=0$ and S_y with $x=0$ bifurcate at primary bifurcation points from the planar interface $x=y=0$. S_y bifurcates subcritically for $n=2$ and supercritically for $n\geq 3$. For certain values of α and β there exists a mixed-mode solution S_m with $x\neq 0$ and $y\neq 0$. For $n=2$ and $n=3$ the secondary bifurcations of S_y and S_x, respectively, become transcritical due to the μ_i terms in (3.11) and S_m develops limit points. The mixed-mode branches S_m always connect the pure-mode solutions S_x and S_y. This implies that after a spatial modulation by the beating of the two modes the solidifying system jumps from a cellular interface with wave number nk_0 to another cellular interface with wave number $(n+1)k_0$ through the mixed-mode branch S_m. This phenomenon is known as mode jumping and is analogous to that observed, e.g., in the buckling of a rectangular plate in the plastic regime when subject to a compressive load.[27]

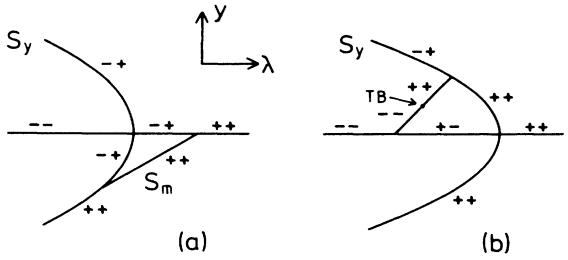

FIG. 13. Diagrams for $n=1$ and (k_0,u) lying on D_1.

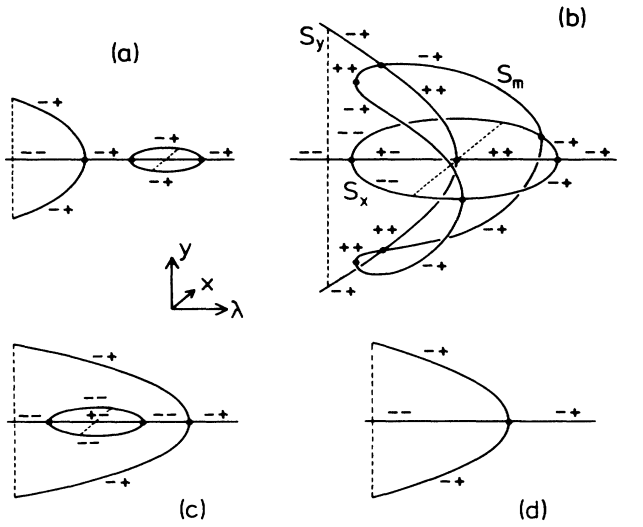

FIG. 14. Qualitatively different diagrams of the unfolded normal form (3.11) for $n=2$ and $(k_0,u)=P_2$.

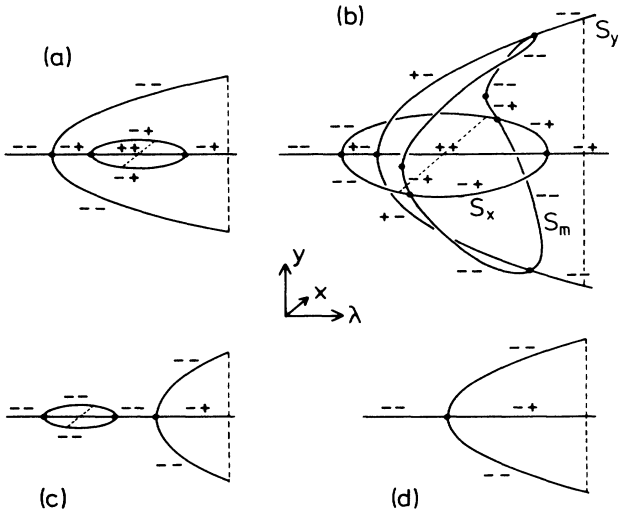

FIG. 15. Same as Fig. 14 for $n=3$ and $(k_0,u)=P_3$.

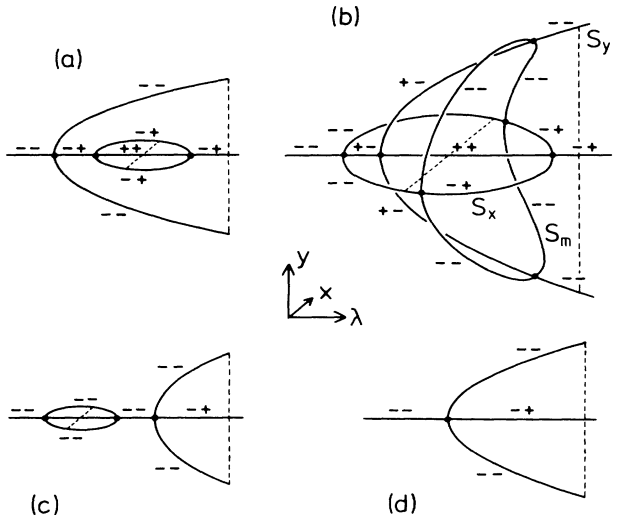

FIG. 16. Same as Fig. 14 for $n \geqq 4$ and $(k_0,u)=P_n$.

IV. CONCLUSION

Several interesting physical consequences for cellular interface bifurcations in a solidifying material can be drawn which are in principle experimentally testable and add new insight to the phenomenology of directional solidification. First, we have condensed all the information that is available from Eqs. (2.2)—(2.6) on the bifurcation to and between stationary cellular interfaces into two unifying equations (3.3) and (3.7) for single-mode and double-mode instabilities. Then, using the method of normal forms, the different bifurcation diagrams, which govern the solidification process near instability threshold have been determined. The way in which the system bifurcates depends on the values of k_0 and u which are known functions of the sample's width, the applied temperature gradient, and of material parameters involved. Thus, different material compositions of the alloy may lead to different types of bifurcations. On the other hand, it is always possible to drive the system into the neighborhood of a desired type of bifurcation. In the case of a single-mode bifurcation, stationary and stable cellular interfaces occur, whose spatial periodicity is determined by the wave number of the critical mode. In particular, there exist bistable and mushroom hysteretic effects and islands. The latter can be reached experimentally by fluctuations that push the system into the island's stability basin. The simultaneous bifurcation of two different modes gives rise to steady-state mode interactions. Here the bifurcation behavior depends sensitively on the wave numbers. The bifurcation diagrams exhibit primary bifurcation to pure-mode solutions and secondary bifurcations to mixed-mode solutions which connect the pure-mode branches. The pure-mode solutions correspond to interfaces with a wavelength given by one of the unstable modes. The mixed-mode branches represent interfaces given by spatial beats of the two wavelengths of the two unstable modes. Furthermore, in some instances, one encounters tertiary bifurcations on the mixed-mode branch which are here Hopf bifurcations to standing waves.

Within the framework of the model equations (2.1)—(2.5) the bifurcation diagrams presented in this paper exhaust all phenomena that can be obtained by a local analysis near the onset of instability. We wish to emphasize, however, that the forms of the bifurcation equations (3.3) for a single unstable mode and of (3.7) for two neighboring unstable modes are generally valid for any solidification system in two dimensions with nonflux boundary conditions at the sidewalls. Consequently, from a topological point of view, the bifurcations realized by such a solidification system must be members of the hierarchy of bifurcation diagrams discussed in Refs. 25 and 22. The special diagrams that we obtained in this paper are due to the special degeneracies imposed by the form of the equations (2.1)—(2.5). If the model is altered but the nonflux boundary conditions and the reflection symmetry are kept [the structure of (2.12b) and (2.13b) then remains], one can expect to obtain more diagrams or other types of diagrams. In particular, it appears that the solidification system considered by Ungar and Brown,[14] where the temperature gradient is used as a bifurcation parameter and a less rigid approximation of the concentration jump at the interface is assumed, may give rise to new types of bifurcations than those found here. It would be of considerable interest to compare these diagrams with the numerical results of these authors. The next steps ought then to consist of an analysis of three dimensional systems and, of course, to submit the phenomena described above to an experimental test.

ACKNOWLEDGMENTS

The author expresses his gratitude to W. Güttinger, G. Dangelmayr, and D. Armbruster for many valuable discussions. This work was supported by the Stiftung Volkswagenwerk (Hannover), Federal Republic of Germany.

APPENDIX

In this appendix we calculate explicitly the most important expressions used above.

(1) We first give the expression for the coefficients $a^{(n)}_{r_1,r_2,\ldots,r_m}$ in Eq. (2.11a). We have

$$a^{(n)}_{r_1,r_2,\ldots r_m}=\frac{1}{\mu(r_1,r_2,\ldots,r_m)}F_m(r_1,r_2,\ldots,r_m)Q(n)$$
$$-\sum_{\eta=0}^{m-1}\sum_{\alpha\in P_\eta(\mathcal{N}_m)}\sum_{(n_1,n_2,\ldots,n_{m-\eta})\in\mathcal{N}_{m\setminus\alpha}}\left[\frac{1}{(m-\eta-1)!}uk_0^2n_1(r_{\alpha_1}+r_{\alpha_2}+\cdots+r_{\alpha_\eta})\right.$$

$$+\frac{1}{(m-\eta)!}Q^2(r_{a_1}+r_{a_2}+\cdots+r_{a_\eta})\Bigg]$$

$$\times(-1)^{m-\eta-1}\frac{1}{\mu(r_{a_1},\ldots,r_{a_\eta})}F_\eta(r_{a_1},r_{a_2},\ldots,r_{a_\eta})Q^{m-\eta-1}(r_{a_1}+r_{a_2}+\cdots+r_{a_\eta}), \quad \text{(A1)}$$

where

$$\sum_{i=1}^{m} r_i=n,\quad P_\eta(\mathbb{N}_m)=\{M\subset\mathbb{N}_m \mid |M|=\eta\},\quad \mathbb{N}_m=\{1,2,3,\ldots,m\}.$$

For $\mathcal{A}\in P_\eta(\mathbb{N}_m)$ we set $\tilde{\mathcal{A}}:=(\tilde{\mathcal{A}}_1,\tilde{\mathcal{A}}_2,\ldots,\tilde{\mathcal{A}}_\eta)$ with $\tilde{\mathcal{A}}_i\in\mathcal{A}$ and $\tilde{\mathcal{A}}_1<\tilde{\mathcal{A}}_2<\ldots<\tilde{\mathcal{A}}_\eta$,

$$M_{\mathcal{A}}:=\{(r_{(\pi\tilde{\mathcal{A}})_1},r_{(\pi\tilde{\mathcal{A}})_2},\ldots,r_{(\pi\tilde{\mathcal{A}})_\eta}) \mid \pi\in S_\eta\},$$

where S_n is the group of permutations of n elements. Furthermore, we have

$$\mu(r_1,r_2,\ldots,r_\eta)=\prod_{r\in\mathcal{R}(r_{\tilde{a}_1},r_{a_2},\ldots,r_{\tilde{a}_\eta})}|J(r;r_1,r_2,\ldots,r_\eta)|!.$$

The quantities entering (A1) are defined by

$$\mathcal{R}(r_1,r_2,\ldots,r_\eta)=\{r_1,r_2,\ldots,r_\eta\}\quad\text{(attention: } r_i=r_j \text{ for } i\neq j\rightarrow |\mathcal{R}|<\eta),$$

$$J(r;r_1,r_2,\ldots,r_\eta)=\{i\in\mathbb{N}_\eta \mid r=r_i\},$$

$$Q(m)=\frac{v}{2}+\left[\frac{v^2}{4}+um^2k_0^2\right]^{1/2},$$

$$F_0(m)=1, F_1(m)=v-1-m^2k_0^2,$$

$$F_m(r_1,r_2,\ldots,r_m)=-(-v)^m-\sum_{\eta=1}^{m-1}\sum_{\alpha\in P_\eta(\mathbb{N}_m)}F_\eta(r_{\tilde{a}_1},r_{\tilde{a}_2},\ldots,r_{\tilde{a}_\eta})[-Q(r_{\tilde{a}_1}+r_{\tilde{a}_2}+\cdots+r_{\tilde{a}_\eta})]^{m-\eta}$$

$$-\tfrac{1}{2}[1+(-1)^{m+1}]u^{(m-1)/2}k_0^{m+1}(r_1+r_2+\cdots+r_m)r_1r_2\cdots r_m\frac{m!!(m-1)!}{\left[\frac{m-1}{2}\right]!2^{(m-1)/2}}.$$

In particular we obtain $a_n^{(n)}=F_1(n)Q(n)-v^2$,

$$a_{2n}^{(2n)}=F_1(2n)Q(2n)-v^2,$$

$$a_{-n,2n}^{(n)}=F_1(2n)Q(n)Q(2n)-F_1(2n)Q^2(2n)+2un^2k_0^2[F_1(n)+F(2n)]-v^2Q(n)+v^3,$$

$$a_{n,n}^{(2n)}=F_1(n)Q(n)Q(2n)-F_1(n)Q^2(n)-un^2k_0^2F_1(n)-\tfrac{1}{2}v^2Q(2n)+\tfrac{1}{2}v^3,$$

$$a_{-n,n,n}^{(n)}=F_1(n)Q^2(n)Q(2n)-F_1(n)Q(n)Q^2(2n)+un^2k_0^2F_1(n)Q(n)$$
$$+2vF_1(n)Q^2(n)+\tfrac{3}{2}un^4k_0^4Q(n)-2v^2F_1(n)Q(n)+\tfrac{1}{2}v^2Q^2(2n)-\tfrac{1}{2}v^2Q(n)Q(2n)-un^2k_0^2v^2-\tfrac{1}{2}v^3Q(n)+\tfrac{1}{2}v^4.$$

(2) The derivatives of B in (2.12) needed for the defining and nondegeneracy conditions can be obtained explicitly in the following way: Suppose that the nth mode is critical. Let $x\equiv\varepsilon_n$ and let (2.11) be represented in the vector form

$$\mathcal{F}(\varepsilon)=(F^{(0)},F^{(1)},F^{(2)},\ldots)=0,$$

$$\varepsilon=(\varepsilon_0,\varepsilon_1,\varepsilon_2,\ldots).$$

Let $G(x)=(\varepsilon_0(x),\varepsilon_1(x),\varepsilon_2(x),\ldots)$ be the solution of

$$\hat{\mathcal{F}}(G(x))=0, \quad \text{(A2)}$$

where

$$\hat{\mathcal{F}}=(F^{(0)},F^{(1)},F^{(2)},\ldots,F^{(n-1)},0,F^{(n+1)},\ldots),$$

which exists by virtue of the implicit function theorem. Then we can write

$$B(x,v)=F^{(n)}(G(x)). \quad \text{(A3)}$$

By differentiation it follows that

$$B_x=\sum_i F_{\varepsilon_i}^{(n)}G_x^{(i)},$$

where subscripts denote partial differentiation. At $x=0$ we have $G(0)=(0,0,\ldots)$, and therefore obtain at $x=0$

$$F^{(n)}_{\varepsilon_n}=a_n,\quad F^{(n)}_{\varepsilon_i}=0 \quad \text{for } i\neq n\ ,$$

which follows from the form of (2.11). From (A2) it follows that

$$\sum_j F^{(i)}_{\varepsilon_j}G^{(j)}_x=0$$

and, therefore, $a_iG^{(i)}_x=0$. For $i=n$ we obtain $G^{(n)}=\varepsilon_n=x$, $G^{(n)}_x=1$. For $i\neq n$ we have $a_i\neq 0$ and thus $G^{(i)}_x=0$. With these results we finally obtain $B_x=a_n$ at $x=0$. Differentiating (A3) further yields

$$B_{xxx}=\sum_{i,j,m} F^{(n)}_{\varepsilon_i\varepsilon_j\varepsilon_m}G^{(i)}_xG^{(j)}_xG^{(m)}_x +3\sum_{i,j}F^{(n)}_{\varepsilon_i\varepsilon_j}G^{(i)}_xG^{(j)}_{xx}+\sum_i F^{(n)}_{\varepsilon_i}G^{(i)}_{xxx}\ . \tag{A4}$$

$F^{(n)}_{\varepsilon_i}$ is nonzero at $\varepsilon=0$ only for $i=n$, but $G^{(n)}_{xxx}=0$. Hence the last series in (A4) vanishes. From (A2) we obtain

$$\sum_{j,m} F^{(i)}_{\varepsilon_j\varepsilon_m}G^{(j)}_xG^{(m)}_x+\sum_j F^{(i)}_{\varepsilon_j}G^{(j)}_{xx}=0,\quad i\neq n\ . \tag{A5}$$

In virtue of $G^{(j)}_x=0$ for $j\neq n$ and $F^{(i)}_{\varepsilon_j}=0$ for $i\neq j$, we are left with

$$F^{(i)}_{\varepsilon_i}G^{(i)}_{xx}=-F^{(i)}_{\varepsilon_n\varepsilon_n}\ . \tag{A6}$$

From (2.11) we infer that $F^{(i)}_{\varepsilon_n\varepsilon_n}$ is different from zero at $\varepsilon=0$ only or $i=0$ or $i=2n$ and with (A1) we obtain

$$F^{(0)}_{\varepsilon_n\varepsilon_n}=-2a^{(0)}_{-n,n}=0\ .$$

Thus it follows from (A6) that

$$G^{(2n)}_{xx}=-2a^{(2n)}_{n,n}/a_{2n},\quad G^{(j)}_{xx}=0 \quad \text{for } j\neq 2n\ .$$

Substituting this into (A4) finally yields Eq. (3.4). By further differentiating the above equations, the derivatives of B at $x=0$ can be calculated to any desired order.

(3) The above calculations can be generalized to the case of two critical modes in a straightforward but tedious manner. For $n\geqq 2$ we obtain

$$B^{(1)}_{xyy}=2(a^{(1)}_1a^{(2n+1)}_{2n+1}a^{(n)}_{-(n+1),n,n+1}-a^{(2n+1)}_{2n+1}a^{(n)}_{-1,n+1}a^{(1)}_{-n,n+1}-a^{(1)}_1a^{(n)}_{-(n+1),2n+1}a^{(2n+1)}_{n,n+1})/(a^{(1)}_1a^{(2n+1)}_{2n+1})\ ,$$

$$B^{(2)}_{xxy}=2(a^{(1)}_1a^{(2n+1)}_{2n+1}a^{(n+1)}_{-n,n,n+1}-a^{(2n+1)}_{2n+1}a^{(n+1)}_{1,n}a^{(1)}_{-n,n+1}-a^{(1)}_1a^{(n+1)}_{-n,2n+1}a^{(2n+1)}_{n,n+1})/(a^{(1)}_1a^{(2n+1)}_{2n+1})\ .$$

(4) The intersection points $P_n=(k^*_n,u^*_n)$ of the curves W_n and Z_n are calculated in the following way. From $a_n=a_{n+1}=0$ it follows with $A=n^2$, $B=(n+1)^2$, and $z=k_0^2$ that

$$Az(v-1-Az)^2u=v^3(1+Az)\ , \tag{A7}$$

$$Bz(v-1-Bz)^2u=v^3(1+Bz)\ , \tag{A8}$$

and for the curve W_n we have

$$u=27(1+Az)^2/(4Az)\ .$$

Solving these three equations for u and z yields

$$k^{*2}_n=2\{B-A-[A(A+3B)]^{1/2}\}/[B(B-5A)]\ ,$$

$$u^*_n=27\{-4A^3-11A^2B-2AB^2+B^3+(-4A^2-5AB+B^2)[A(A+3B)]^{1/2}\}/[8AB(B-5A)]\ .$$

It is then easily seen that

$$\lim_{n\to\infty}k^{*2}_n=0,\quad \lim_{n\to\infty}u^*_n=27\ .$$

From (A7) and (A8) we obtain the critical value v_c of v, viz.,

$$v_c=(1+Az)(1+Bz)+[AzBz(1+Az)(1+Bz)]^{1/2}\ .$$

[1]Phys. Scr. T 9 (special issue, *The Physics of Chaos and Related Problems*, edited by S. Lundquist).

[2]Physica 12D (1984) (special issue, *Fronts, Interfaces and Patterns*, edited by A. R. Bishop, L. J. Campbell, and P. J. Channel).

[3]J. S. Langer, Rev. Mod. Phys. **52**, 1 (1980).

[4]G. Nicolis and J. Prigogine, *Self-Organization in Nonequilibrium Systems* (Wiley, New York, 1977).

[5]R. Thom, *Structural Stability and Morphogenesis* (Benjamin, Reading, MA, 1975); H. Haken, *Synergetics* (Springer, Berlin, 1977); *Advanced Synergetics* (Springer, Berlin, 1983).

[6]D. J. Wollkind and L. A. Segel, Philos. Trans. R. Soc. London **268**, 351 (1970).

[7]W. W. Mullins and R. F. Sekerka, J. Appl. Phys. **34**, 323 (1963); **35**, 444 (1964).

[8]J. S. Langer and L. A. Turski, Acta Metall. **25**, 1113 (1977).

[9]J. S. Langer, Acta Metall. **25**, 1121 (1977).
[10]D. J. Wollkind, R. Srinanganathan, and D. B. Oulton, Physica **12D**, 215 (1984); B. Caroli, C. Caroli, and B. Roulet, J. Phys. (Paris) **43**, 1767 (1982); J. Cryst. Growth **68**, 677 (1984); A. Karma and N. Goldenfeld, Phys. Rev. B **31**, 7018 (1985).
[11]J. S. Langer and H. Müller-Krumbhaar, Phys. Rev. A **27**, 499 (1983); B. Caroli, C. Caroli, B. Roulet, and J. S. Langer, *ibid.* **33**, 442 (1986), R. C. Brower, D. A. Kessler, J. Koplik, and H. Levine, *ibid.* **29**, 1335 (1984); D. A. Kessler, J. Koplik, and H. Levine, *ibid.* **30**, 3161 (1984); **31**, 1712 (1985); E. Ben-Jacob, N. Goldenfeld, J. S. Langer, and G. Schön, *ibid.* **29**, 330 (1984).
[12]M. Kerszberg, Phys. Rev. B **27**, 6796 (1983); Physica **12D**, 262 (1984).
[13]G. B. McFadden and S. R. Coriell, Physica **12D**, 253 (1984).
[14]L. H. Ungar and R. A. Brown, Phys. Rev. B **29**, 1367 (1984); **30**, 3993 (1984); **31**, 5931 (1985); L. H. Ungar, M. J. Bennett, and R. A. Brown, *ibid.* **31**, 5923 (1985).
[15]R. Trivedi and K. Somboonsuk, Mater. Sci. Eng. **65**, 65 (1984).
[16]M. E. Glicksman, Mater. Sci. Eng. **65**, 45 (1984).
[17]F. Heslot and A. Libchaber, Phys. Scr. **T9**, 126 (1985).
[18]M. Golubitsky and D. Schaeffer, Commun. Pure Appl. Math. **32**, 21 (1979); Commun. Math. Phys. **67**, 205 (1979).
[19]M. Golubitsky and D. Schaeffer, *Singularities and Groups in Bifurcation Theory* (Springer, New York, 1985), Vol. I.
[20]P. Haug, Ph.D. Thesis, University of Tübingen, 1987.
[21]H. Fujii, M. Mimura, and Y. Nishiura, Physica **5D**, 1 (1982).
[22]D. Armbruster and G. Dangelmayr, Math. Proc. Cambridge Philos. Soc. **101**, 167 (1987).
[23]G. Dangelmayr and D. Armbruster, in *Contemporary Mathematics* **56**, edited by J. Guckenheimer and M. Golubitsky (American Mathematical Society, Providence, 1986), in press.
[24]W. Güttinger, in *Frontiers in Equilibrium Statistical Physics,* edited by G. T. Moore and M. O. Scully (Plenum, New York, 1986); Ch. Geiger, W. Güttinger, and P. Haug, in *Complex Systems—Operational Approaches,* edited by H. Haken (Springer, Berlin, 1985).
[25]M. Golubitsky and W. F. Langford, J. Differ. Equ. **41**, 375 (1981).
[26]D. Armbuster, G. Dangelmayr, and W. Güttinger, Physica **16D**, 99 (1985).
[27]D. Schaeffer and M. Golubitsky, Commun. Math. Phys. **69**, 209 (1979).